Metrological Characterization of a Signal Generator for the Testing of Medium-Voltage Measurement Transducers

Marco Faifer, *Member, IEEE*, Roberto Ottoboni, *Fellow, IEEE*, Sergio Toscani, *Member, IEEE,* Claudio Cherbaucich, and Paolo Mazza, *Member, IEEE*

I. Introduction

NOWADAYS, the measurement of the electrical quantities in power systems is a task that is performed by exploiting analog to digital conversion and proper signal processing techniques. It is well known that the impact of the necessary electronic stages on the measurement accuracy is small, being almost completely limited by the employed transducers. While the throughput and the resolution of the analog–digital converters, as well as the processing capability of the CPUs and DSPs, have both impressively grown in the last years, the performance of voltage and current transducers has not increased so much.

A specific example is given by the measurement of power and energy in medium-voltage (MV) distribution systems, where sophisticated electronic units are usually employed, both at the level of substation and final user. Despite these units can measure many quantities (voltages, currents, active and reactive power, harmonics, and so on) ensuring an intrinsic accuracy better than 0.1%, the overall uncertainty of the measurement chain is higher because of the current and voltage transducers, which in most cases are conventional voltage and current measurement transformers. Altough their performances are outperformed by modern transducers, among their strengths there are high reliability, safety, low cost and robustness.

Voltage and current transducers are usually characterized in sinusoidal steady-state conditions [1], and therefore their measurement performance can be expressed by means of two parameters: 1) ratio and 2) phase errors [2]–[5]. However, because of the continuously growing number of power electronic converters, and nonlinear and time-varying loads and generators, the level of voltage and current distortion has significantly increased in the past few years. This is especially true in low-voltage distribution networks, but nowadays even considering that MV networks operate in sinusoidal steady conditions is a fairly rough approximation. At the same time, industries increased the awareness that a poor voltage quality reduces their efficiency and productivity, other than increasing the transformers and lines losses, reducing the reliability of the components, triggering resonances, and so on from the distribution system operator's point of view [6]–[8].

Power quality assessment requires high-performance current and voltage transducers [9], which in particular should guarantee adequate accuracy in the presence of multitone signals. When focusing on voltage transducers, the usual approach assumes that it can be considered linear time invariant (LTI), so that it can be characterized by its frequency response function (FRF) [10]–[12], which in turn can be easily measured, for example, by changing the frequency of a sinusoidal excitation. Since transducers such as measurement transformers may exhibit a nonlinear behavior [13], [14], an accurate characterization should be based on the complex test signals. The possibility to generate these complex voltage waveforms is extremely important even for the validation of models of voltage transformers, which considers the nonlinear behavior [15]–[17]. However, this requires a device able to generate multitone waveform of adequate amplitude. Often, a system made of a signal generator, a power amplifier, and a step-up transformer is employed [11], [18]. However, the waveform applied to the device under test may be very different from the output voltage of the signal generator. A more detailed study of the behavior of the voltage transducer

Manuscript received August 4, 2014; revised November 13, 2014; accepted November 18, 2014. Date of publication December 18, 2014; date of current version June 5, 2015. The Associate Editor coordinating the review process was Dr. Edoardo Fiorucci.

M. Faifer, R. Ottoboni, and S. Toscani are with the Dipartimento di Elettrotecnica, Politecnico di Milano, Milan 20133, Italy (e-mail: marco.faifer@polimi.it).

C. Cherbaucich and P. Mazza are with RSE S.p.A., Milan 20134, Italy.

Color versions of one or more of the figures in this paper are available online.

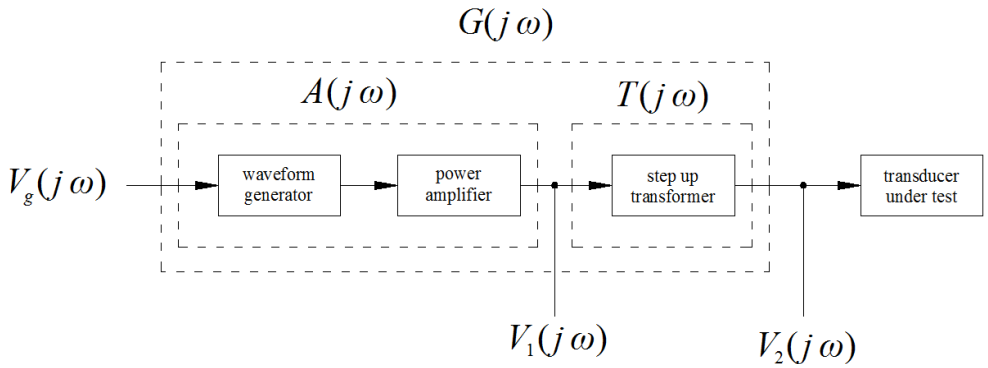

Fig. 1. Block diagram of the MV generator.

would be possible if the test waveform could be accurately controlled; only few and very expensive generators capable of doing this are available on the market. Faifer *et al.* [19] have developed an MV signal generator, which is based on the classical architecture (signal generator, power amplifier, and step-up transformer) but uses a digital compensation of the FRF to improve the performance. The MV generator can be used as the source for the digital comparator presented in [2], and its accuracy in generating voltage waveforms similar to those present in actual MV networks has been evaluated [20]. In this paper, a deeper analysis of the metrological performance of the signal generator is provided. In particular, the most significant uncertainty sources have been identified and their contributions have been evaluated. Since it will be shown that the nonlinear effects are not negligible, the uncertainty of the generator strictly depends on the spectral content of the voltage to be generated. A specific case has been studied in this paper; however, the approach is general, and therefore it can be applied by considering signals having a different spectral distribution.

Section II briefly describes the signal generator proposed by the authors. Section III presents the characterization procedure. The test setup is detailed in Section IV, while the experimental results are reported and discussed in Section V. Finally, the conclusion is given in Section VI.

II. Medium-Voltage Generator

As discussed during the introduction, the characterization of MV transducers in nonsinusoidal conditions requires equipment allowing to generate complex test voltages. In many cases, the simple setup shown in Fig. 1 is employed for the purpose. It consists of a waveform generator connected to the input of a power amplifier, which in turns feeds the low-voltage winding of a proper step-up transformer. The transducer under test measures the voltage across the secondary winding of the step-up transformer. Having supposed to neglect nonlinear phenomena, both the power amplifier and the step-up transformer behave essentially like bandpass filters. Unfortunately, in most cases, some of their zeros and poles fall in the frequency range from few hertz to some kilohertz, which is the most interesting for the testing of the voltage transducers, where the spectral components of the test signal lie. For this reason, the user cannot accurately control the test voltage waveform v_2, since its relationship with v_g, namely, the reference of the waveform generator, cannot be expressed by a simple scale factor.

On the contrary, having hypothesized that the system can be well approximated by an LTI model, it is completely characterized by its frequency response and can be represented by the block diagram shown in Fig. 1. Therefore, when periodic steady-state conditions are considered, it can be written

$$V_2(j\omega) \cong G(j\omega)V_g(j\omega) \tag{1}$$

where $V_2(j\omega)$ and $V_g(j\omega)$ are the spectra of the secondary voltage and the reference voltage of the waveform generator. It is clear that if an estimate $G_{\text{est}}(j\omega)$ of the FRF $G(j\omega)$ is available, it is possible to compute $V_{gr}(j\omega)$, which is the spectrum of the signal to be applied to the input of the power amplifier to obtain the desired spectrum of the output voltage $V_{2_r}(j\omega)$. Therefore, it is possible to employ the conventional test setup shown in Fig. 1 while having an accurate control of the voltage applied to the transducer under test

$$V_{gr}(j\omega) = \frac{V_{2r}(j\omega)}{G_{\text{est}}(j\omega)}. \tag{2}$$

Since both the power amplifier and the step-up transformer have a nonzero output impedance, their input–output relationship depends on the electrical load, hence on the voltage transducer to be tested. Therefore, in general, $G_{\text{est}}(j\omega)$ has to be measured every time the voltage transducer under test has changed. The authors have developed an MV generator based on this simple prefiltering technique [19]. Nonlinear effects have been supposed to be negligible if the output voltage v_1 of the power amplifier remains below its maximum rated peak voltage V_{ap} and if the absolute value of the magnetic flux in the iron core φ is lower than its rated peak value Φ_{pn}. These conditions have to be verified during the estimation of the FRF $G(j\omega)$ and also before starting the generation of the desired output voltage v_{2r}.

Checking the first condition requires predicting the voltage across the primary winding of the step-up transformer to obtain the desired output voltage. For this reason, it is important to also measure the FRF $T(j\omega)$ between the secondary and the primary voltage of the transformer

$$V_{1r}(j\omega) = \frac{V_{2r}(j\omega)}{T_{\text{est}}(j\omega)} \tag{3}$$

where $V_{1r}(j\omega)$ is the predicted spectrum of the voltage applied to the primary winding and $T_{\text{est}}(j\omega)$ is the estimated FRF between the secondary and the primary voltage of the transformer.

The second check can be performed by assuming that the voltage drop across the secondary winding is negligible. In this case, the magnetic flux in the core is equal to the secondary winding flux linkage, divided by the number of secondary turns. Hence, the condition is verified if the absolute value of ψ_{2e}, namely, the integral of the secondary voltage (which represents an estimation of the secondary flux linkage) is lower than $\Psi_{2\text{pn}}$, which is the rated peak flux linkage of the secondary winding. It is quite easy to check if the magnetic flux remains lower than Φ_{pn} since ψ_{2e} can be obtained by integrating v_{2r} and then compared with $\Psi_{2\text{pn}}$.

III. Characterization of the Voltage Generator

The target of this paper is analyzing the performance of the voltage generator described in the previous section, and in particular, investigating how the FRF $G_{\text{est}}(j\omega)$ affects them. Generally speaking, it is clear that the accuracy of the voltage generation depends on how well $G_{\text{est}}(j\omega)$ describes the input–output relationship of the system. Differences between the desired and the actual secondary voltage are the results of the uncertainty of $G_{\text{est}}(j\omega)$, which is basically due to two contributions. First of all, the estimation of the FRF is based on a measurement process, which is inevitably affected by measurement uncertainty. Then, there is another important uncertainty source in the process that can be called definitional uncertainty. In fact, the technique treats the system as perfectly LTI, but unfortunately it is not, thus resulting in an additional uncertainty source. While the accuracy of $G_{\text{est}}(j\omega)$ is crucial, that of $T(j\omega)$ is much less critical since it is just needed to check whether the primary voltage is compatible with the capabilities of the power amplifier and of the step-up transformer. Therefore, it will not be discussed in detail.

A. Harmonic Distortion Test

The first step for the characterization of the voltage generator is investigating whether the nonlinear phenomena are relevant or not. A very simple test to detect and quantify the amount of harmonic distortion, and hence to evaluate the impact of the nonlinearities, would be programming the arbitrary waveform generator to inject a so-called odd–odd multisine signal [21]. Basically, its output voltage v_g is a periodic signal having a fundamental frequency f_0 and only its harmonics of order $k_h = 4m+1$, where m is a positive integer lower than $m_{\max}$. Furthermore, the odd–odd excitation allows distinguishing between even and odd harmonic distortion. In fact, the spectral components of the measured voltages at the frequencies $(4m+2)\omega_0$ are due to even harmonic distortion only, while those having frequencies given by $(4m+3)\omega_0$ are produced by odd harmonic distortion only.

Let us call $V_g(jk_h\omega_0)$ the spectrum of v_g. The level of the signal should be set so that the estimated secondary winding flux linkage reaches $\Psi_{2\text{pn}}$, which is its peak value in rated conditions. In this way, the peak of the magnetic flux of the transformer is near its rated value, thus magnifying the nonlinearities due to core saturation, which is likely to be the major cause of harmonic distortion. Assuming that the system does not generate subharmonics, after the transient components have faded out, both the primary and secondary voltages of the step-up transformer are periodic and have the same fundamental frequency f_0 of the excitation signal. N periods of the two signals have to be acquired, and let us call $V_{1h}^{[i]}(jk_h\omega_0)$ and $V_{2h}^{[i]}(jk_h\omega_0)$ the spectra of the ith period of the primary and of the secondary voltage, respectively. Under these conditions, it is possible to compute the average of the spectral components and their standard deviations by exploiting the data of each of the N periods

$$V_{1h,\text{avg}}(jk_h\omega_0) = \frac{1}{N}\sum_{i=1}^{N} V_{1h}^{[i]}(jk_h\omega_0)$$
$$V_{2h,\text{avg}}(jk_h\omega_0) = \frac{1}{N}\sum_{i=1}^{N} V_{2h}^{[i]}(jk_h\omega_0) \tag{4}$$

$$s_{V1h,\text{avg}}(jk_h\omega_0) = \sqrt{\frac{1}{N(N-1)}\sum_{i=1}^{N}\left|V_{1h}^{[i]}(jk_h\omega_0) - V_{1h\text{avg}}(jk_h\omega_0)\right|^2}$$
$$s_{V2h,\text{avg}}(jk_h\omega_0) = \sqrt{\frac{1}{N(N-1)}\sum_{i=1}^{N}\left|V_{2h}^{[i]}(jk_h\omega_0) - V_{2h,\text{avg}}(jk_h\omega_0)\right|^2}. \tag{5}$$

The standard deviations $s_{V1h,\text{avg}}(jk_h\omega_0)$ and $s_{V2h,\text{avg}}(jk_h\omega_0)$ are the estimates of the uncertainty of the spectral components, assuming that it is essentially due to zero-mean noise. Therefore, if the amplitude of the nonexcited components in the two spectra is much higher than their standard deviation, it can be concluded that the system produces nonlinear distortion.

B. Single-Shot Estimation of the Frequency Response Functions

If the impact of the nonlinear distortion is low enough, then it seems reasonable to model the MV generation system by means of the FRFs $G(j\omega)$ and $T(j\omega)$. The choice of the stimulus signal, which is the voltage v_g, is extremely important for this purpose. In fact, it is well known that best results can be achieved with a periodic excitation [21]. It is also important that the excitation signal has the same fundamental frequency ω_0 and contains the components having frequencies given by $k_l\omega_0$, which are at least the same of the signal to be generated. In this way, once having obtained an estimate of the FRF $G(j\omega)$ at the frequencies of interest, the voltage to be set in the waveform generator to obtain the desired secondary voltage can be computed using (2) without introducing further uncertainty due to frequency interpolation. The measurements of the FRFs require acquiring N periods of the voltages v_1 and v_2, which are the steady-state response of the stimulus signal v_g. The spectra acquired during the N periods have

$$s_{G,e}(jk_l\omega_0) = \frac{s_{V2,\text{avg}}(jk_l\omega_0)}{|V_g(jk_l\omega_0)|}$$

$$s_{T,e}(jk_l\omega_0) = |T_e(jk_l\omega_0)|\sqrt{\frac{s^2_{V1,\text{avg}}(jk_l\omega_0)}{|V_{1,\text{avg}}(jk_l\omega_0)|^2} + \frac{s^2_{V2,\text{avg}}(jk_l\omega_0)}{|V_{2,\text{avg}}(jk_l\omega_0)|^2} - 2\Re\left[\frac{s^2_{V1,V2,\text{avg}}(jk_l\omega_0)}{V_{1,\text{avg}}(jk_l\omega_0)V^*_{2,\text{avg}}(jk_l\omega_0)}\right]}. \quad (8)$$

to be averaged, thus obtaining $V_{1,\text{avg}}(jk_l\omega_0)$ $V_{1,\text{avg}}(jk_l\omega_0)$; the FRFs can be estimated as

$$G_e(jk_l\omega_0) = \frac{V_{2,\text{avg}}(jk_l\omega_0)}{V_g(jk_l\omega_0)}$$
$$T_e(jk_l\omega_0) = \frac{V_{2,\text{avg}}(jk_l\omega_0)}{V_{1,\text{avg}}(jk_l\omega_0)}. \quad (6)$$

$V_g(jk_l\omega_0)$ is the spectrum of the stimulus signal v_g. $G_e(jk_l\omega_0)$ and $T_e(jk_l\omega_0)$ are the maximum likelihood estimations if the measurements are affected by zero-mean Gaussian noise. Using (5), it is possible to compute the standard deviations $s_{V1,\text{avg}}(jk_l\omega_0)$ and $s_{V2,\text{avg}}(jk_l\omega_0)$, while the covariance $s^2_{V1,V2,\text{avg}}(jk_l\omega_0)$ of the spectra can be estimated as usual

$$s^2_{V1,V2,\text{avg}}(jk_l\omega_0) = \frac{1}{N(N-1)}\sum_{i=1}^{N}\left[V_1^{[i]}(jk_l\omega_0) - V_{1,\text{avg}}(jk_l\omega_0)\right] \cdot\left[V_2^{[i]}(jk_l\omega_0) - V_{2,\text{avg}}(jk_l\omega_0)\right]^* \quad (7)$$

where * denotes complex conjugation.

Finally, the standard deviations of the two FRFs result in (8), as shown at the top of this page. It is worth reminding that the formula for estimating the standard deviation of $T_e(jk_l\omega_0)$ has been reported for the sake of completeness. Since this FRF is employed just to predict whether the maximum voltage output of the power amplifier will be exceeded to obtain the desired voltage across the transducer under test, its accuracy is not critical.

C. Effect of Remanent Magnetization

The standard deviation $s_{V1,\text{avg}}(jk_l\omega_0)$ can be used to estimate the uncertainty contribution due to the noise, but it does not consider that measuring $G(j\omega)$ means representing a nonlinear system with a linear model. This aspect requires further investigations. Other than harmonic distortion, the behavior of the voltage generator may suffer from another more complex nonlinearity: the magnetic hysteresis of the iron core. A hysteretic behavior means that the steady-state response of the system also depends on the history, which in this case is represented by the remanence of the transformer core. It is clear that a proper degaussing procedure can be used to eliminate the residual magnetic flux, but the employment of the voltage generator becomes more complicated. A very simple method can be employed to evaluate the impact of the residual flux on the measurement of $G(j\omega)$, hence on the accuracy of the voltage generation. Basically, the estimation of $G(j\omega)$ has to be repeated M times using the same periodic stimulus signal, whose spectrum is $V_g(jk_l\omega_0)$. In each experiment, after the acquisition process has been completed, the generation of the excitation signal has to be interrupted after a random time between zero and a period. For each repetition r (where $r = 1, \ldots, M$), using the N observed periods, an FRF $G_e^{[r]}(jk_l\omega_0)$ and its sample standard deviation $s^{[r]}_{G,e}(jk_l\omega_0)$ can be obtained by applying the usual formulas. From these data, other interesting quantities can be computed

$$G_{eR}(jk_l\omega_0) = \frac{1}{M}\sum_{r=1}^{M} G_e^{[r]}(jk_l\omega_0)$$
$$s_{G,eR}(jk_l\omega_0) = \sqrt{\frac{1}{M(M-1)}\sum_{r=1}^{M}\left|G_e^{[r]}(jk_l\omega_0) - G_{eR}(jk_l\omega_0)\right|^2} \quad (9)$$
$$s_{G,eR,n}(jk_l\omega_0) = \frac{1}{M}\sqrt{\sum_{r=1}^{M} s^{2[r]}_{G,e}(jk_l\omega_0)}$$

where $G_{eR}(jk_l\omega_0)$ is the average of the FRFs measured during the M repetitions. If the system was perfectly LTI, it should be almost equal to the FRFs estimated during each experiment, since the slight differences are due to the measurement noise. The statement remains true even if the system produces harmonic distortion, since even in this case, the steady-state response to an excitation signal just depends on the signal itself. However, if the relationship between v_g and v_2 suffers from significant time variance or dynamic nonlinearities (such as hysteresis), $G_{eR}(jk_l\omega_0)$ may differ from the FRFs evaluated during each repetition, and this difference may be so large that it cannot be attributed just to the noise during the measurement process. $s_{G,eR}(jk_l\omega_0)$ is the total sample standard deviation of $G_{eR}(jk_l\omega_0)$. The scattering of the FRF evaluated during the several repetitions, and therefore the value of $s_{G,eR}(jk_l\omega_0)$, is due to the noise, to the time variance (which can be excluded), and possibly to complex nonlinearities. On the contrary, $s_{G,eR,n}(jk_l\omega_0)$ is the sample noise standard deviation, which just depends on the noise in the measurement process. It is clear that if the system is LTI or just affected by harmonic distortion, the expectations of $s_{G,eR}(jk_l\omega_0)$ and $s_{G,eR,n}(jk_l\omega_0)$ are equal, while the effect of remanence may make the first considerably higher than the latter.

D. Measurement of the Best Linear Approximation

Once having analyzed the nonlinear effects of the system, the proposed approach requires evaluating the FRF $G_{\text{BLA}}(j\omega)$, which better describes the relationship between the reference voltage of the waveform generator and the secondary voltage,

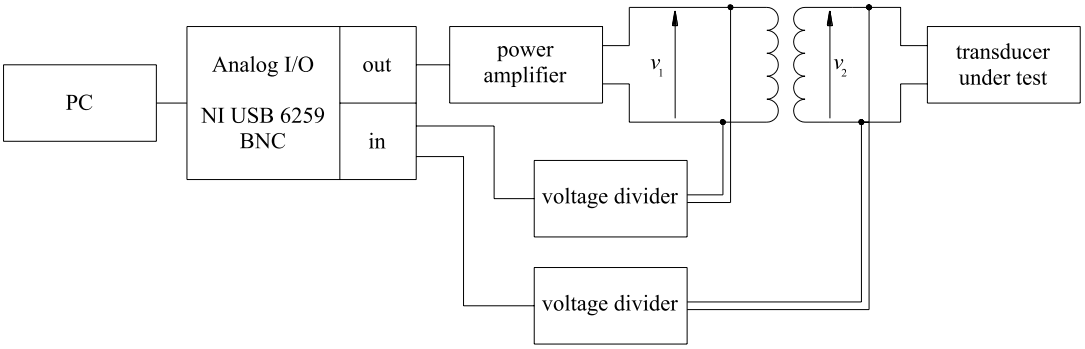

Fig. 2. Experimental setup.

thus optimizing the accuracy of the MV generator. Formally

$$G_{\mathrm{BLA}}(j\omega) = \arg\min E\left(|v_2(t) - v_{2r}(t)|^2\right). \tag{10}$$

$G_{\mathrm{BLA}}(j\omega)$ is the so-called best linear approximation (BLA) of the system [22]. It is well known that $G_{\mathrm{BLA}}(j\omega)$ depends on the power spectrum of the (periodic) input signal. However, evaluating the BLA of the system for a given power spectrum is rather simple. The stimulus signal v_g is a random multisine having a fundamental frequency ω_0: as usual, the FRF can be estimated by measuring N periods of the steady-state response of the system, and computing the ratio between the average spectrum of the secondary voltage and that of the stimulus signal. This experiment has to be repeated M times by randomly changing the phases of the spectral components of the stimulus signal. For each repetition r, the average spectra $V_g^{[\mathrm{r}]}(jk_l\omega_0)$ and $V_2^{[\mathrm{r}]}(jk_l\omega_0)$ of the input and output signals, respectively, and the average FRF $G_e^{[r]}(jk_l\omega_0)$ as well as its standard deviation $s_{G,e}^{[r]}(jk_l\omega_0)$ can be evaluated. Furthermore, it is possible to compute

$$G_{\mathrm{BLA}}(jk_l\omega_0) = \frac{1}{M}\sum_{r=1}^{M} G_e^{[r]}(jk_l\omega_0)$$

$$s_{G,\mathrm{BLA}}(jk_l\omega_0) = \sqrt{\frac{1}{M(M-1)}\sum_{r=1}^{M}\left|G_e^{[r]}(jk_l\omega_0) - G_{\mathrm{BLA}}(jk_l\omega_0)\right|^2} \tag{11}$$

$$s_{G,\mathrm{BLA},n}(jk_l\omega_0) = \frac{1}{M}\sqrt{\sum_{r=1}^{M} s_{G,e}^{2[r]}(jk_l\omega_0)}.$$

$G_{\mathrm{BLA}}(jk_l\omega_0)$ is the estimation of the BLA, computed as the average between the FRFs evaluated in each of the M random phase realizations. $s_{G,\mathrm{BLA}}(jk_l\omega_0)$ is the sample standard deviation of the BLA, which is due to the combined effect of nonlinearities (both to remanence, which is different for each random phase realization, and to the stochastic nonlinear distortions) and noise. Basically, $s_{G,\mathrm{BLA}}(jk_l\omega_0)$ evaluates the accuracy of the developed MV generator for a given power spectra of the input signal. $s_{G,\mathrm{BLA},n}(jk_l\omega_0)$ is the sample standard deviation due to noise; if the system was perfectly LTI, the expectations of $s_{G,\mathrm{BLA}}(jk_l\omega_0)$ and $s_{G,\mathrm{BLA},n}(jk_l\omega_0)$ would be equal. Finally, it would be interesting to estimate the standard uncertainty σ_V of the voltage generator. Basically, it is the square root of the expectation of the difference between the actual and the desired secondary voltage spectra

$$\sigma_V(j\omega) = \sqrt{E\left(|V_2(j\omega) - V_{2r}(j\omega)|^2\right)}. \tag{12}$$

Using the sample standard deviation estimator

$$s_V(jk_l\omega_0) = \sqrt{\frac{1}{M-1}\sum_{r=1}^{M}\left|V_2^{[r]}(jk_l\omega_0) - V_{2r}^{[r]}(jk_l\omega_0)\right|^2} \tag{13}$$

where

$$\begin{aligned} V_2^{[r]}(jk_l\omega_0) &= G_e^{[r]}(jk_l\omega_0)V_g^{[r]}(jk_l\omega_0) \\ V_{2r}^{[r]}(jk_l\omega_0) &= G_{\mathrm{BLA}}(jk_l\omega_0)V_g^{[r]}(jk_l\omega_0). \end{aligned} \tag{14}$$

Substituting

$$s_V(jk_l\omega_0) = \sqrt{\frac{1}{M-1}\sum_{r=1}^{M}\left|V_g^{[r]}(jk_l\omega_0)\right|^2\left|G_e^{[r]}(jk_l\omega_0) - G_{\mathrm{BLA}}(jk_l\omega_0)\right|^2}. \tag{15}$$

Since the power spectrum of v_{gr} is constant

$$s_V(jk_l\omega_0) = \sqrt{M}|V_g(jk_l\omega_0)|s_{G,\mathrm{BLA}}(jk_l\omega_0). \tag{16}$$

Assuming that the difference between the spectra of the actual and the desired secondary voltage is small, the most interesting relative standard deviation results in

$$\frac{s_V(jk_l\omega_0)}{|V_{2r}(jk_l\omega_0)|} = \sqrt{M}\frac{s_{G,\mathrm{BLA}}(jk_l\omega_0)}{|G_{\mathrm{BLA}}(jk_l\omega_0)|}. \tag{17}$$

The expression represents a very easy method to evaluate the relative standard uncertainty of the generator in the frequency domain. It exploits the same data used to compute the BLA of the system.

IV. Experimental Setup

The characterization procedure described in the previous section has been applied to an MV generator previously developed by the authors using the experimental setup shown in Fig. 2.

The MV generator consists of a power amplifier with adjustable gain (its main characteristics are reported in Table I) whose output is connected to the low-voltage winding of a

TABLE I
SPECIFICATIONS OF THE POWER AMPLIFIER

Parameter	Values
Maximum output voltage	140 V
Voltage gain	Continuously variable from -∞ to 34 dB
-3dB bandwidth	5 Hz-50 kHz
Signal to noise ratio	-100 dB
THD (8 Ω load)	Less than 0.02% below rated output voltage

100 V/5 kV transformer having a rated frequency of 50 Hz. The method requires to feed the input of the power amplifier with arbitrary waveforms and to measure the voltage across the two windings of the step-up transformer. The generation and the acquisition of the voltage signals are synchronized since both of them have been performed using a National Instruments NI USB-6259 board with a maximum aggregate sampling rate of 1 Msample/s, 16-b resolution, and an input range of ±5 V. Wideband voltage dividers have been employed as voltage transducers, while the management of the data acquisition and waveform generation as well as the processing and analysis of the measurement data has been implemented in MATLAB. A 15-pF capacitor has been connected to the high-voltage side of the step-up transformer to emulate the loading effect of a capacitive voltage divider that has to be tested.

V. EXPERIMENTAL RESULTS

The aim of the first test is evaluating the significance of the nonlinear phenomena and, in particular, the generation of harmonic distortion. An odd–odd random phase multisine excitation signal with a fundamental frequency of 1 Hz and a maximum frequency of 10 kHz has been employed. The peak amplitude of the stimulus signal has been normalized to fit the dynamic range of the analog output channel, and an adequately high sampling frequency of 200 kHz has been chosen. The gain of the power amplifier has been initially set to a very low value, and then the generation of the excitation signal has been started. After that, the gain of the amplifier has been increased so that the secondary voltage reached about 3.3 kV, well below the maximum voltage rating. Having verified that the initial transient components have been damped, $N = 10$ periods of the primary and secondary voltages have been acquired. The secondary winding flux linkage can be easily estimated by integrating the secondary voltage; its peak amplitude is about 22.8 Wb, which is close to that reached in rated conditions (22.5 Wb). The spectra of the acquired voltages and their standard deviations computed according to (5) are depicted in Figs. 3 and 4.

Fig. 3 reports the spectrum of the voltage at the secondary side of the step-up transformer. The amplitudes of almost

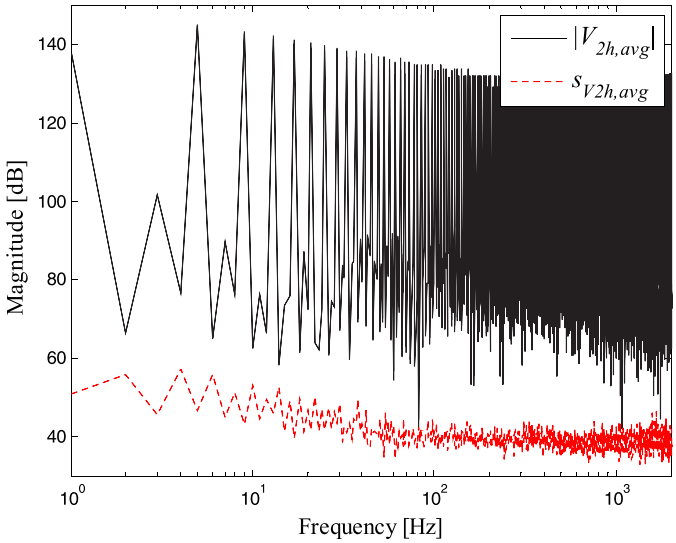

Fig. 3. Spectrum of the secondary voltage with odd–odd multisine excitation and its standard deviation.

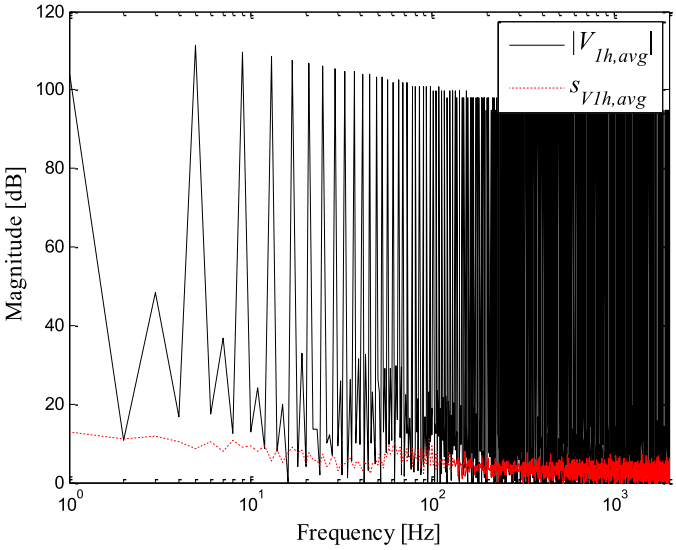

Fig. 4. Spectrum of the primary voltage with odd–odd multisine excitation and its standard deviation.

all of the nonexcited harmonics are substantially higher than their standard deviations; therefore, they are produced by the nonlinearities of the system. The amplitudes of the nonexcited components in the secondary voltage with respect to the fundamental are relatively high, especially at the low frequencies; for example, the highest nonexcited component (namely the third) is about 36 dB lower than the fundamental. Fig. 4 shows the spectrum of the primary voltage and its sample standard deviation. Even in this case, most of the nonexcited components (especially at the left side of the spectrum) are much higher than their sample standard deviations. It should be noted that the amount of harmonic distortion is significantly lower than that of the secondary voltage; in fact, the highest nonexcited component (again the third harmonic) is about 60 dB lower than the fundamental. The reason is

that the main cause of nonlinearity is due to the distorted magnetizing current drawn by the step-up transformer, which produces noticeable effects even when the magnetic flux is around its rated value. The consequent voltage drop across the output impedance of the power amplifier produces harmonic distortion in the primary voltage, while the voltage drop across the low-voltage winding series impedance causes further distortion in the secondary voltage. The output impedance of the amplifier is generally much lower than the primary winding series impedance; therefore, harmonic distortion is considerably stronger in the secondary voltage. Distortion caused by core saturation mainly produces odd nonlinearities; as expected, the previous figures show that the amplitudes of the nonexcited even harmonics are lower than those of the odd harmonic components.

From this preliminary test, it can be concluded that the generation system produces a moderate amount of harmonic distortion, and therefore it appears that its behavior can be adequately described by the FRFs $G(j\omega)$ and $T(j\omega)$ defined in the previous sections. Now, these FRFs have to be measured in the frequency range of interest, which goes from $f_{\min} = 1$ Hz to $f_{\max} = 10$ kHz. A compensated quasi-logarithmic random phase excitation has been chosen [23]. This signal is periodic but has a spectral power density, which is very similar to that of pink noise; therefore, it is particularly suitable for identifying the system in a frequency range of several decades. The fundamental angular frequency of the signal is $\omega_0 = 2\pi f_{\min}$, while k_l is the order of the generic harmonic component contained in the excitation. A sampling frequency of 200 kHz has been chosen, and the stimulus signal has been built starting from a 200 points per decade frequency grid. After the generation of the stimulus signal has been started and the transient components have been faded out, $N = 10$ periods of the primary and secondary voltages have been acquired. The secondary voltage reached about 3 kV, while the peak value of the secondary winding flux linkage was about 22.5 Wb, hence very close to its rated value. Once the data acquisition process has been completed, $G_e(jk_l\omega_0)$, $T_e(jk_l\omega_0)$, and their standard deviations $s_{G,e}(jk_l\omega_0)$ and $s_{T,e}(jk_l\omega_0)$ can be estimated using (6) and (8), thus obtaining the graphs shown in Figs. 5 and 6. The FRF $T_e(jk_l\omega_0)$ between the secondary and the primary voltage of the step-up transformer appears that of a low-pass filter; the reason is that the high-pass effect due to the core magnetization is not visible in the frequency range of interest. A large resonance peak located at about 3.6 kHz can be clearly noticed, and many others can be detected by extending the measurement to higher frequencies. They are due to the interaction between the winding inductances, the parasitic capacitances, and the 15-pF capacitor, which simulates the electrical load of the capacitive voltage divider to be tested. $G_e(jk_l\omega_0)$ has a bandpass behavior: the low-frequency part is due to the ac coupling filter of the power amplifier, which is intended for audio applications. On the contrary, the shape of the high-frequency part of $G_e(jk_l\omega_0)$ is very close to that of $T_e(jk_l\omega_0)$, since the frequency response of the power amplifier is pretty flat in this range. The values of the sample standard deviations $s_{G,e}(jk_l\omega_0)$ and $s_{T,e}(jk_l\omega_0)$, which are due to the noise in the measurement channels, are quite low. In fact, both the relative amplitudes of $s_{G,e}(jk_l\omega_0)$ and $s_{T,e}(jk_l\omega_0)$ are lower than -70 dB in the frequency range 1 Hz–10 kHz, and they fall below -85 dB between 10 Hz and 2 kHz.

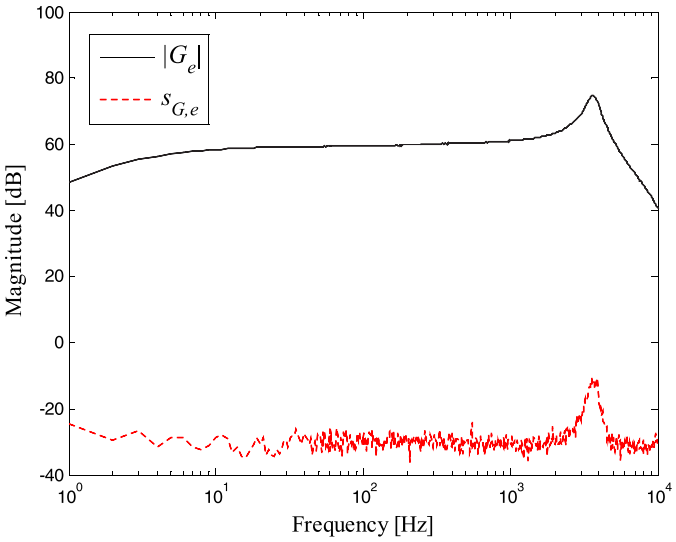

Fig. 5. Estimation of $G(jk_l\omega_0)$ and its standard deviation.

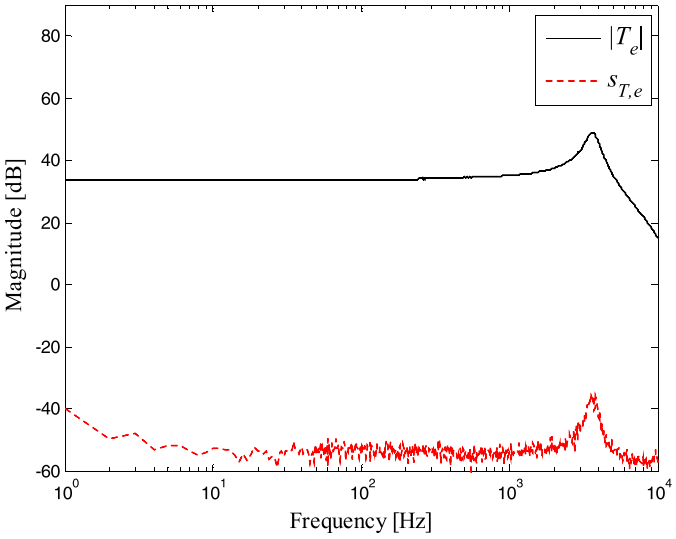

Fig. 6. Estimation of $T(jk_l\omega_0)$ and its standard deviation.

As shown during the harmonic distortion test, the main source of nonlinearity arises from the magnetization characteristic of the step-up transformer, which is affected by hysteresis other than saturation. The impact of remanence on the estimation of the FRF $G(j\omega)$ can be evaluated using the procedure described in Section III. Therefore, the measurement of $G(j\omega)$ in the conditions described in the previous section has been repeated for $M = 20$ times using the same excitation signal. For each measurement, the generation of the stimulus signal has been stopped after a random time, considering a uniform probability density function between zero and $1/f_{\min}$. For each repetition, the FRF $G_e^{[r]}(jk_l\omega_0)$ and its sample standard deviation $s_{G,e}^{[r]}(jk_l\omega_0)$ can be evaluated. Using (9), it is possible

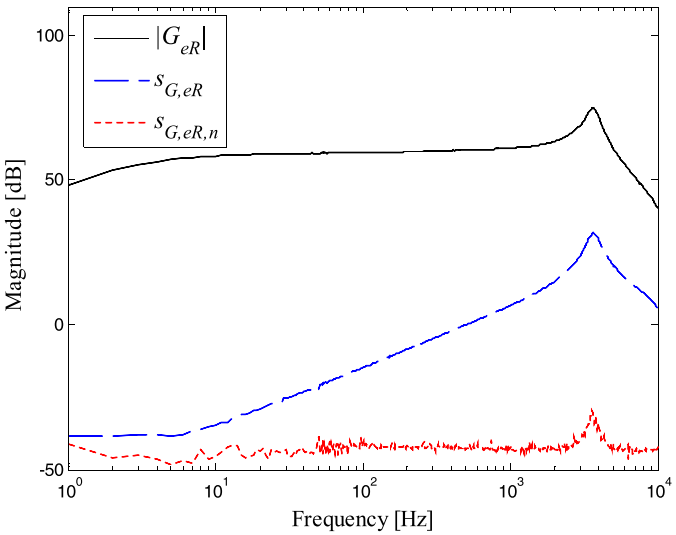

Fig. 7. Multiple estimations of $G(j\omega)$ using the same excitation signal: average frequency response, total sample standard deviation, and noise sample standard deviation.

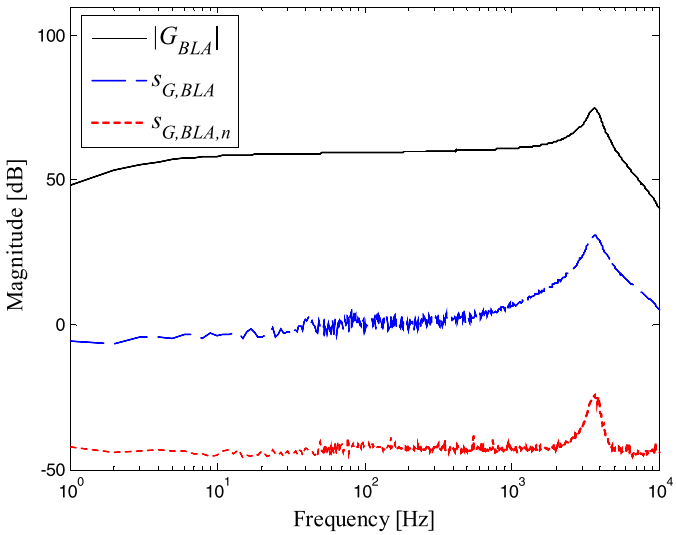

Fig. 8. BLA of the system, the total sample standard deviation, and the noise sample standard deviation.

to compute the average FRF $G_{eR}(jk_l\omega_0)$, the total sample standard deviation $s_{G,eR}(jk_l\omega_0)$, and the noise sample standard deviation $s_{G,eR,n}(jk_l\omega_0)$. The results are shown in Fig. 7.

At low frequencies, $s_{G,eR}(jk_l\omega_0)$ and $s_{G,eR,n}(jk_l\omega_0)$ are very close, and their relative amplitude is lower than -80 dB. However, at the higher frequencies, the total sample standard deviation is much greater than the noise sample standard deviation, being the latter up to 60 dB higher. In particular, the relative total sample standard deviation rises to -45 dB near the resonance peak. Therefore, the most significant effect of the residual magnetic flux appears as a slight change of the measured FRF, especially near the high-frequency resonance peak. Even if quite small, this phenomenon is clearly noticeable with the employed measurement setup and may significantly affect the performance of the signal generator.

After having evaluated the impact of remanence on the estimation of the FRF $G(j\omega)$, which is moderate although considerably higher than the measurement accuracy, it is possible to compute the BLA of the system. The BLA of the system is the FRF that minimizes the mean square error between the actual and the predicted output, for a given spectral content of the input signal. The BLA of the system has been evaluated using a compensated quasi-logarithmic multisine excitation. The estimation of the transfer function $G(j\omega)$ has been repeated $M = 20$ times in the usual conditions, but using different random phase realizations. The BLA $G_{\mathrm{BLA}}(jk_l\omega_0)$, the total sample standard deviation $s_{G,\mathrm{BLA}}(jk_l\omega_0)$, and the noise sample standard deviation $s_{G,\mathrm{BLA},n}(jk_l\omega_0)$ can be computed according to (11). Finally, (17) shows how to estimate the relative standard uncertainty of the signal generator in these conditions. The results are summarized in Figs. 8 and 9.

From Fig. 8, it can be clearly seen that the total sample standard deviation is much higher than the noise sample standard deviation over the whole considered frequency range, thus indicating the presence of noticeable nonlinear phenomena. When compared with Fig. 7, the total sample

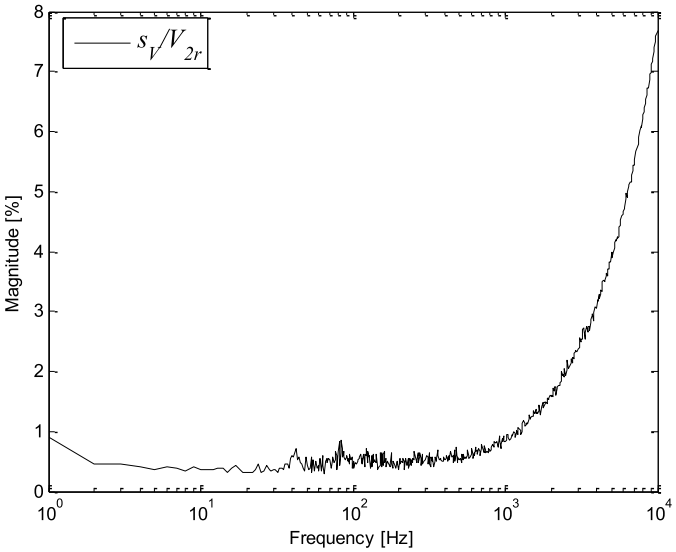

Fig. 9. Relative standard uncertainty of the voltage generator.

standard deviations are very close at the higher frequencies, since the relative total sample standard deviation is again -45 dB near the resonance peak. However, the new total sample standard deviation is much higher in the right part of the spectrum, because of the effect of the stochastic nonlinear distortions due to the random phase realizations. Therefore, it can be concluded that the measurement of the FRF is mainly affected by harmonic distortion at the lower frequencies and by the remanent magnetization near the resonance peak.

Fig. 9 reports the relative standard uncertainty of the voltage generator when the signal v_g is a compensated quasi-logarithmic multisine. It remains below 1% from 1 Hz to 1.2 kHz, thus ensuring good performance over the most important frequency range for the testing of voltage transducers. When restricting the range from 2 to 500 Hz, the standard uncertainty becomes lower than 0.5%. However, the accuracy becomes much worse in the rightmost part of

the spectrum, being about 7.5% at 10 kHz. In this range, the FRF contains resonances which are affected by the remanent magnetic field. Because of the high slope of the FRF in both magnitude and phase, these small variations result in a high uncertainty. Finally, it should be noticed that the characterization has been carried out using a compensated quasi-logarithmic multisine excitation. However, the method is general and can be applied using other class of excitations.

VI. Conclusion

The authors have recentely proposed an MV generator for testing transducers with complex waveforms, thus allowing to apply specific test signals in order to evaluate their performance in conditions that are similar to those found in real MV networks. The basic architecture is conventional, being made of a signal generator, a power amplifier, and a step-up transformer, but the performance is enhanced through digital compensation of the FRF. In this paper, a deep analysis of this voltage generator has been carried out, and, in particular, the effectiveness of the frequency response compensation. The impact of nonlinear phenomena (such as harmonic distortion and remancence) on the accuracy of the voltage generation has been evaluated using a periodic signal having a spectral content similar to that of pink noise. It can be concluded that the harmonic distortion is the major responsible for the uncertainty at low frequencies, while hysteresis is more relevant at a frequency higher than 1 kHz. Since the uncertainty is related to nonlinear effects, it strongly depends on the spectrum of the signal to be generated. However, the proposed approach is general and can be applied considering different harmonic contents. Furthermore, since this paper clearly indicates what the main sources of uncertainty are, it also suggests how the performance of the generator can be improved, for example, using a feedforward compensation, which employs a nonlinear model instead of a simple FRF.

References

[1] *Instrument Transformers—Part 3: Additional Requirements for Inductive Voltage Transformers*, IEC Standard 61869-1, 2007.

[2] A. Brandolini, M. Faifer, and R. Ottoboni, "A simple method for the calibration of traditional and electronic measurement current and voltage transformers," *IEEE Trans. Instrum. Meas.*, vol. 58, no. 5, pp. 1345–1353, May 2009.

[3] M. Faifer, R. Ottoboni, and S. Toscani, "Electronic combined transformer for power-quality measurements in high-voltage systems," *IEEE Trans. Instrum. Meas.*, vol. 60, no. 6, pp. 2007–2013, Jun. 2011.

[4] M. Faifer and R. Ottoboni, "An electronic current transformer based on Rogowski coil," in *Proc. IEEE Int. Instrum. Meas. Technol. Conf.*, Victoria, BC, Canada, May 2008, pp. 1554–1559.

[5] G. Crotti, D. Giordano, and A. Sardi, "Development and use of a medium voltage RC divider for on-site calibration," in *Proc. IEEE Int. Workshop Appl. Meas. Power Syst.*, Aachen, Germany, Sep. 2011, pp. 53–57.

[6] J. Arrillaga and N. R. Watson, *Power System Harmonics*, 2nd ed. New York, NY, USA: Wiley, 2003.

[7] I. Hunter, "Power quality issues—A distribution company perspective," *Power Eng. J.*, vol. 15, no. 2, pp. 75–80, Apr. 2001.

[8] M. Radmehr, S. Farhangi, and A. Nasiri, "The power of paper—Effects of power quality distortions on electrical drives and trasformer life in paper industries," *IEEE Ind. Appl. Mag.*, vol. 13, no. 5, pp. 38–48, Sep./Oct. 2007.

[9] C. Muscas, "Power quality monitoring in modern electric distribution systems," *IEEE Instrum. Meas. Mag.*, vol. 13, no. 5, pp. 19–27, Oct. 2010.

[10] G. Olivier, R.-P. Bouchard, Y. Gervais, and D. Mukhedkar, "Frequency response of HV test transformers and the associated measurement problems," *IEEE Trans. Power App. Syst.*, vol. PAS-99, no. 1, pp. 141–146, Jan./Feb. 1980.

[11] S. Zhao, H. Y. Li, P. Crossley, and F. Ghassemi, "Testing and modelling of voltage transformer for high order harmonic measurement," in *Proc. Int. Conf. Electr. Utility Deregulation Restruct. Power Technol.*, Weihai, China, Jul. 2011, pp. 229–233.

[12] M. Klatt, J. Meyer, M. Elst, and P. Schegner, "Frequency responses of MV voltage transformers in the range of 50 Hz to 10 kHz," in *Proc. Int. Conf. Harmon. Quality Power*, Bergamo, Italy, Sep. 2010, pp. 1–6.

[13] R. Stiegler, J. Meyer, and P. Schegner, "Portable measurement system for the frequency response of voltage transformers," in *Proc. IEEE Int. Conf. Harmon. Quality Power*, Hong Kong, Jun. 2012, pp. 745–750.

[14] N. Locci, C. Muscas, and S. Sulis, "Experimental comparison of MV voltage transducers for power quality applications," in *Proc. IEEE Int. Instrum. Meas. Technol. Conf.*, Singapore, May 2009, pp. 92–97.

[15] F. D. Torre *et al.*, "Instrument transformers: A different approach to their modeling," in *Proc. IEEE Int. Workshop Appl. Meas. Power Syst.*, Aachen, Germany, Sep. 2011, pp. 37–42.

[16] A. Rezaei-Zare, R. Iravani, and M. Sanaye-Pasand, "Impacts of transformer core hysteresis formation on stability domain of ferroresonance modes," *IEEE Trans. Power Del.*, vol. 24, no. 1, pp. 177–186, Jan. 2009.

[17] Y. Baghzouz and X. D. Gong, "Voltage-dependent model for teaching transformer core nonlinearity," *IEEE Trans. Power Syst.*, vol. 8, no. 2, pp. 746–752, May 1993.

[18] H. Tatizawa, E. S. Neto, G. F. Burani, A. A. C. Arruda, K. T. Soletto, and N. M. Matsuo, "Calibration of high voltage transducers for power quality measurements in electric networks," in *Proc. Power Qual.*, 2011, pp. 237–254. [Online]. Available: http://www.intechopen.com/books/power-quality

[19] M. Faifer, R. Ottoboni, S. Toscani, C. Cherbaucich, M. Gentili, and P. Mazza, "A medium voltage signal generator for the testing of voltage measurement transducers," in *Proc. IEEE Int. Instrum. Meas. Technol. Conf.*, Minneapolis, MN, USA, May 2013, pp. 194–199.

[20] M. Faifer, R. Ottoboni, S. Toscani, P. Mazza, and C. Cherbaucich, "Characterization of an arbitrary medium voltage signal generator," in *Proc. IEEE Int. Instrum. Meas. Technol. Conf.*, Montevideo, Uruguay, May 2014, pp. 143–148.

[21] R. Pintelon and J. Schoukens, *System Identification: A Frequency Domain Approach*, 2nd ed. Boston, MA, USA: Wiley, 2012.

[22] L. Lauwers, "Some applications of the best linear approximation in nonlinear block-oriented modelling," Ph.D. dissertation, Dept. Fundam. Elect. Instrum., Vrije Univ., Brussel, Belgium, 2011.

[23] E. Geerardyn, Y. Rolain, and J. Schoukens, "Design of quasi-logarithmic multisine excitations for robust broad frequency band measurements," in *Proc. IEEE Int. Instrum. Meas. Technol. Conf.*, Graz, Austria, May 2012, pp. 737–741.